University of South Florida
Scholar Commons

Marine Science Faculty Publications | College of Marine Science

3-15-1999

Response of the West Florida Shelf Circulation to Climatological Wind Stress Forcing

H. J. Yang

Robert H. Weisberg
University of South Florida, weisberg@marine.usf.edu

Follow this and additional works at: http://scholarcommons.usf.edu/msc_facpub

Part of the Marine Biology Commons

Scholar Commons Citation
Yang, H. J. and Weisberg, Robert H., "Response of the West Florida Shelf Circulation to Climatological Wind Stress Forcing" (1999). *Marine Science Faculty Publications.* Paper 125.
http://scholarcommons.usf.edu/msc_facpub/125

This Article is brought to you for free and open access by the College of Marine Science at Scholar Commons. It has been accepted for inclusion in Marine Science Faculty Publications by an authorized administrator of Scholar Commons. For more information, please contact scholarcommons@usf.edu.

JOURNAL OF GEOPHYSICAL RESEARCH, VOL. 104, NO. C3, PAGES 5301–5320, MARCH 15, 1999

Response of the West Florida Shelf circulation to climatological wind stress forcing

Huijun Yang and Robert H. Weisberg

Department of Marine Science, University of South Florida, St. Petersburg

Abstract. The response of the west Florida continental shelf circulation to monthly mean climatological wind forcing is investigated by using the three-dimensional, primitive equation Princeton Ocean Model. Two basic seasonal patterns of circulation and sea surface elevation occur under a barotropic setting: a winter pattern from October to March and a summer pattern from April to September. An interesting finding in winter is an anticyclonic gyre over the northeastern (Florida Big Bend) region that merges with a northwestward flow from the south. The Big Bend Gyre is caused by a convergence of two separate flows: a nearshore along-shelf southeastward flow and an offshore northwestward flow. Winter circulation characteristics also include offshore surface transport, coastal upwelling, and relatively low coastal sea level. The summer pattern features a continuous northwestward directed flow, onshore surface transport, coastal downwelling, and relatively high coastal sea level. Transitions between the two seasonal patterns show either a development or relaxation of the Big Bend Gyre. These three-dimensional circulation patterns result from wind-driven Ekman transports and their resulting surface-slope-induced geostrophic flows. Qualitative agreement exists in some respects with recent in situ observations, historical drift bottle retrievals, and tide gauge data. However, climatological wind stress forcing alone does not account for the seasonally varying southeastward currents observed at midshelf. Thus it may be concluded that for depths less than 50m the seasonal winds may play a dominant role in the seasonal variation of the shelf circulation; and beyond this limit seasonal density related effect must also be a factor in the seasonally varying circulation on the West Florida Shelf.

1. Introduction

The west Florida continental shelf (Figure 1) is characterized by broad, gently sloping topography that extends approximately 200 km from the coast to the shelf break. It is semienclosed, bounded by the Florida Keys in the south and the Florida panhandle in the north. The shelf circulation is subject to the seasonally varying wind stress, buoyancy inputs, and the influence of the Loop Current that enters the Gulf of Mexico through the Yucatan Channel and exists as the Gulf Stream through the Florida Strait.

Many important biological phenomena occur within the West Florida Shelf region that may be related to the circulation. These include episodic, seasonal blooms of (red tide) toxic dinoflagellates thought to originate at midshelf [*Steidinger*, 1983; *Vargo et al.*, 1987], the seasonal formation of high-concentration pigment plumes near the shelf break [*Gilbes et al.*, 1996], and the seasonal succession of fisheries' recruitment. Despite the potential importance of the circulation in determining water properties and for promoting organism growth and distribution, relatively little is known about the annual cycle of the west Florida continental shelf circulation.

Low-frequency variations of the circulation near the shelf break over the southern portion of the region were noted by *Niiler* [1976] and *Maul* [1977] in relation to the Loop Current. However, it is unlikely that a direct influence of the Loop Current can extend to the midshelf or inner shelf. Drift bottle release studies from the middle portion of the West Florida Shelf [*Tolbert and Salsman*, 1964; *Williams et al.*, 1977] suggested a seasonality in the surface circulation evidenced by returns to the north for releases in summer versus returns to the south for releases in winter. Recently, relatively long term in situ current measurements at midshelf [*Weisberg et al.*, 1996] confirmed that seasonal reversals in the circulation do occur. Others have documented shorter term observations of the responses of the midshelf and inner shelf currents and sea level to synoptic scale weather forcing [e.g., *Mitchum and Sturges*, 1982; *Blaha and Sturges*, 1981; *Cragg et al.*, 1983; *Marmorino*, 1982; *Mitchum and Clarke*, 1986].

Copyright 1999 by the American Geophysical Union.

Paper number 1998JC900101.
0148-0227/99/1998JC900101$09.00

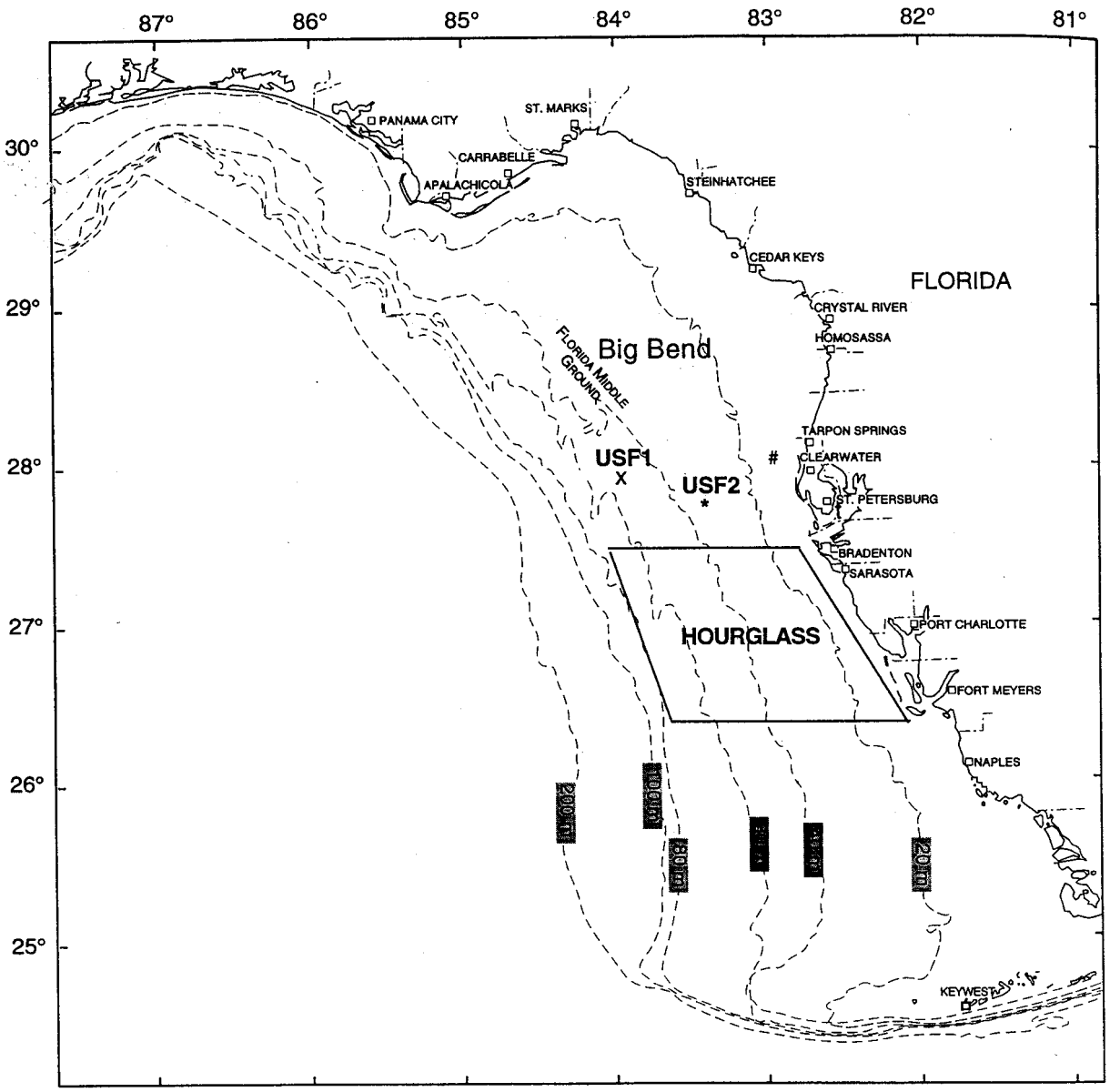

Figure 1. Bathymetric map of the West Florida Shelf region and model domain. USF1 and USF2 are two University of South Florida buoy locations at 28°N, 84°W and 27° 49'N, 83° 25'W, indicated by a cross and star, respectively. A tide gauge station is located inside of Tampa Bay at St. Petersburg, indicated by "t". The drifter release area of the Hourglass project is indicated by the region between Tampa Bay to Fort. Myers to the 73 m isobath. An off Clearwater coastal location is also indicated by number symbol.

While the Gulf of Mexico in its entirety has been the topic of several numerical model studies [e.g., *Oey*, 1995], only two such studies exist for the West Florida Shelf. *Hsueh et al.* [1982] investigated the responses to a prototypical winter storm using a linearized, barotropic storm-surge model. *Cooper* [1987] applied a linearized, three dimensional model to investigate the wind-driven seasonal response but with very coarse horizontal resolution and unrealistic coastal geometry. Neither of these studies offers evidence of seasonal variations. Most full Gulf of Mexico numerical models do not adequately resolve the West Florida Shelf circulation, and no evidence has been offered for the seasonal variations over the shelf.

Motivated by direct observations of systematic, seasonal variations in the west Florida Shelf currents and sea level, this paper provides a numerical investigation of the response of the west Florida continental shelf to seasonally varying, climatologically averaged monthly wind stress forcing. The primary goals are to estimate the seasonal pattern of the West Florida Shelf circulation attributable to the climatological wind forcing

alone and to determine whether or not these patterns can explain the seasonal current reversal found at mid-shelf. To provide high spatial resolution with realistic topography and coastal geometry, and to consider the fully three dimensional flow fields, we have applied the public domain, primitive equation Princeton Ocean Model (POM). Section 2 discusses the model application. Section 3 first discusses the anticyclonic gyre observed in the model results over the northeastern region in late fall and winter. The results of 12 model runs to quasi steady state are then presented, one for each of the climatological monthly mean wind fields of *Hellerman and Rosenstein* [1983]. Comparisons with data are made in section 4, followed by a summary in section 5.

2. Description of the Model

2.1. Model Formulation

Our main interest herein is the large-scale low-frequency shelf water response to climatological monthly wind forcing. *Clarke and Brink* [1985] showed that the response is mainly barotropic and confined to the shelf when $|N\alpha/f| << 1$, where N is the shelf-averaged buoyancy frequency, f is Coriolis parameter and α is the average shelf slope. On the West Florida Shelf for winter, N is about 10^{-3}, α is 5×10^{-4}, and $f = 6.6 \times 10^{-5} s^{-1}$. These values give $|N\alpha/f| < 10^{-2} << 1$, so that the wind-driven response is expected to be barotropic on the West Florida Shelf [*Mitchum and Clarke*, 1986]. We thus begin by considering the barotropi response of the shelf circulation.

Three features of the POM, as developed and described in detail by *Blumberg and Mellor* [1983, 1987], made it an appropriate choice for this study. First, the model uses a sigma coordinate system in the vertical, so it can be applied with realistic shelf topography. Second, along with a mode-splitting technique, where the depth-averaged and the depth-dependent circulations are solved separately, the model allows the free surface elevation to be calculated prognostically. Third, vertical mixing processes evolve with the flow field using the turbulence closure model of *Mellor and Yamada* [1982].

The model domain for the west Florida continental shelf application (Figure 1) includes the region from 87^oW to 81^oW and 24^oN to 30.3^oN. From south to north, the shelf broadens within the Florida Big Bend region between Clearwater and Apalachicola Bay. It then narrows along the Florida panhandle. These regional differences in geometry have an important influence on the circulation. For subsequent comparisons between model results and observations, Figure 1 also gives the locations of two in situ current meter stations (USF1 and USF2), an off Clearwater coastal location, the location of the St. Petersburg tide gauge, and the region of drift bottle releases from the Hourglass Experiment [*Williams et al.*, 1977].

The basic equations are cast in a bottom-following, sigma coordinate system, $\sigma = (z - \eta)/(H + \eta)$, where $H(x, y)$ is the bottom topography; η is the sea surface elevation; and x,y, z are the conventional Cartesian coordinates. Thus σ ranges from 0 at the sea surface ($z = \eta$) to -1 at the seafloor ($z = -H$).

The equations governing the shelf circulation and the surface elevation are

$$\frac{\partial(DU)}{\partial x} + \frac{\partial(DV)}{\partial y} + \frac{\partial \omega}{\partial \sigma} + \frac{\partial \eta}{\partial t} = 0 \qquad (1)$$

$$\frac{\partial(UD)}{\partial t} + \frac{\partial(UUD)}{\partial x} + \frac{\partial(UVD)}{\partial y} + \frac{\partial(U\omega)}{\partial \sigma} - fVD + gD\frac{\partial \eta}{\partial x} = \frac{\partial}{\partial \sigma}\left[\frac{K_M}{D}\frac{\partial U}{\partial \sigma}\right] + F_x \qquad (2)$$

$$\frac{\partial(VD)}{\partial t} + \frac{\partial(UVD)}{\partial x} + \frac{\partial(VVD)}{\partial y} + \frac{\partial(V\omega)}{\partial \sigma} + fUD + gD\frac{\partial \eta}{\partial y} = \frac{\partial}{\partial \sigma}\left[\frac{K_M}{D}\frac{\partial V}{\partial \sigma}\right] + F_y \qquad (3)$$

where the density is assumed to be constant; U, V are horizontal velocity components; ω is the vertical velocity component normal to the sigma surface; $D = H + \eta$; K_M is a variable vertical kinematic viscosity modeled according to the level 2.5 turbulence closure scheme of *Mellor and Yamada* [1982]; f is the Coriolis parameter; g is the acceleration due to gravity; and F_x and F_y are the horizontal friction terms, defined as

$$F_x = \frac{\partial}{\partial x}(D\tau_{xx}) + \frac{\partial}{\partial y}(D\tau_{yx}) \qquad (4)$$

$$F_y = \frac{\partial}{\partial x}(D\tau_{xy}) + \frac{\partial}{\partial y}(D\tau_{yy}) \qquad (5)$$

where

$$\tau_{xx} = 2A_M\frac{\partial U}{\partial x}$$

$$\tau_{xy} = \tau_{yx} = A_M(\frac{\partial U}{\partial y} + \frac{\partial V}{\partial x})$$

$$\tau_{yy} = 2A_M\frac{\partial V}{\partial y}$$

and A_M is the horizontal viscosity modeled according to the Smagorinsky formulation:

$$A_M = C\Delta x\Delta y\left[(\frac{\partial U}{\partial x})^2 + (\frac{\partial V}{\partial y})^2 + (\frac{\partial U}{\partial y} + \frac{\partial V}{\partial x})^2\right]$$

where C is a constant taken to be 0.2.

The model uses an Arakawa C grid conserving both linear and quadratic quantities such as mass and energy. Time differencing is explicit in the horizontal and implicit in the vertical. The implicit time differencing removes the time step constraints on the vertical spacing and allows fine resolution near the sea surface and seafloor. Time integration is split into a two-dimensional external mode, with a short time step,

and a three-dimensional internal mode, with a long time step, based on the Courant-Friedrichs-Levy (CFL) condition. The external mode equations are obtained by integrating the internal model equations (1)-(3) over depth, to eliminate all vertical structure.

The boundary conditions in the vertical are both kinematical and dynamical. Thus $\omega = 0$ at the sea surface and seafloor ($\sigma = 0,\ -1$). At the sea surface, U and V are related to the wind stress components τ^x, τ^y by

$$\frac{K_M}{D}\left(\frac{\partial U}{\partial \sigma}, \frac{\partial V}{\partial \sigma}\right) = \frac{1}{\rho_0}(\tau^x,\ \tau^y),\ \sigma \to 0 \qquad (6)$$

where ρ_0 is the water density. At the seafloor, the horizontal velocity components are zero and the vertical shear is specified by

$$\frac{K_M}{D}\left(\frac{\partial U}{\partial \sigma}, \frac{\partial V}{\partial \sigma}\right) = C_z\sqrt{U^2+V^2}(U,V),\ \sigma \to -1 \quad (7)$$

where

$$C_Z = \mathrm{Max}\left\{\frac{k^2}{[\ln(1+\sigma_{kb-1}H/z_0)]^2}, 0.0025\right\},$$

$k = 0.4$ is the von Karman constant, z_0 is the roughness parameter, and $kb-1$ is the vertical level next to the seafloor. Thus, while the sea surface stress is specified, the bottom stress is determined internally within the model. From a state of rest, the surface motion is first driven by the specified surface wind stress. This generates an interior flow through the pressure gradient and the vertical mixing of momentum according to the *Mellor and Yamada* [1982] turbulence closure scheme. The motion near the sea floor then generates the bottom stress by (7) with the velocity equal to zero at the seafloor.

The horizontal boundary conditions over the land in the north and east are implemented by a land mask, which ensures that the velocity over the land and the normal velocity along the coast line are zero. The model domain has open boundaries in the south, west, and east over water. The depth-averaged transports normal to these boundaries are specified to be zero. That is,

$$\int_{-1}^{0} U\,d\sigma = 0$$

on the western and eastern boundaries over water and

$$\int_{-1}^{0} V\,d\sigma = 0$$

on the southern boundary. Thus there are no net horizontal transports into or out of the domain, so the total water mass within the domain is always conserved. However, depth-dependent flows occur into or out of the domain across the open boundaries according to a Sommerfield radiation condition [*Orlanski*, 1976]. For example, on the western open boundary, the radiation boundary condition is simply

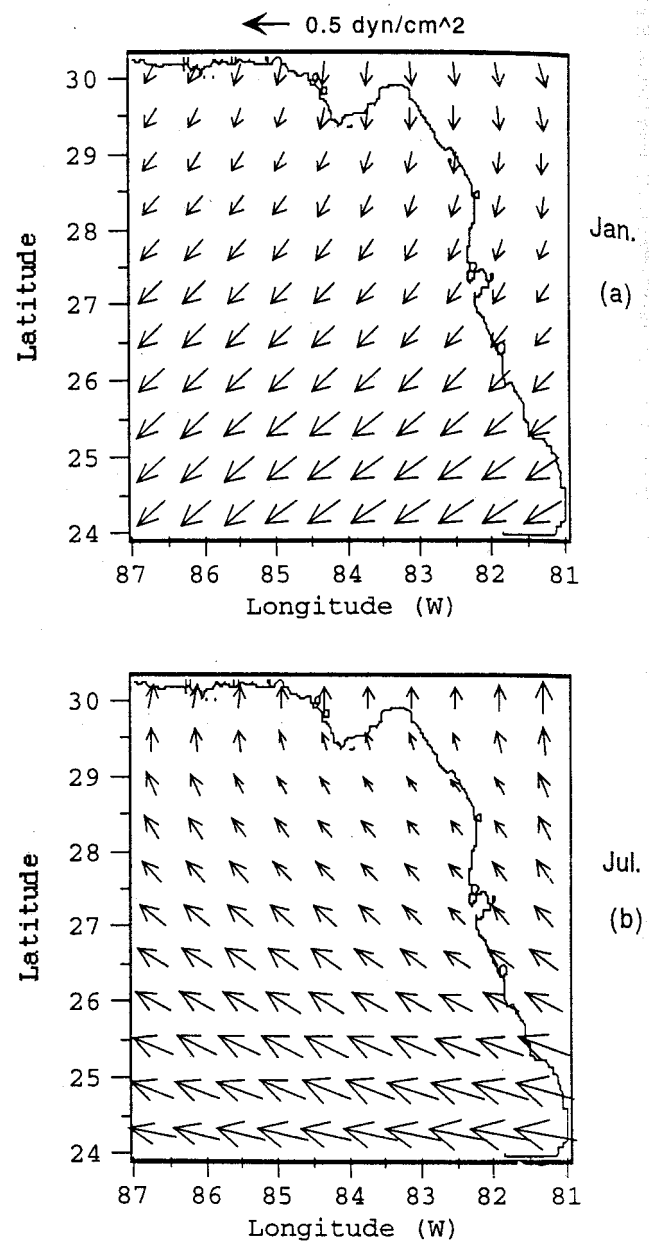

Figure 2. Hellerman and Rosenstein [1983] climatological wind stress fields in (a) January and (b) July.

$$\frac{\partial U}{\partial t} - C_i\frac{\partial U}{\partial x} = 0.$$

Here, C_i, the gravity wave speed, is equal to $\sqrt{gH}$. Similar boundary conditions are applied to the eastern and southern boundaries.

In this application, an evenly spaced 4.6 km rectangular horizontal grid is used to resolve the circulation with 21 levels in the vertical, where the vertical spacing is nonuniform to provide higher resolution within the surface and bottom boundary layers. The maximum depth is assumed to be 1500 m and the minimum water depth is 5 m. Tests with different maximum water depth show little effect on the shelf circulation pattern. The sur-

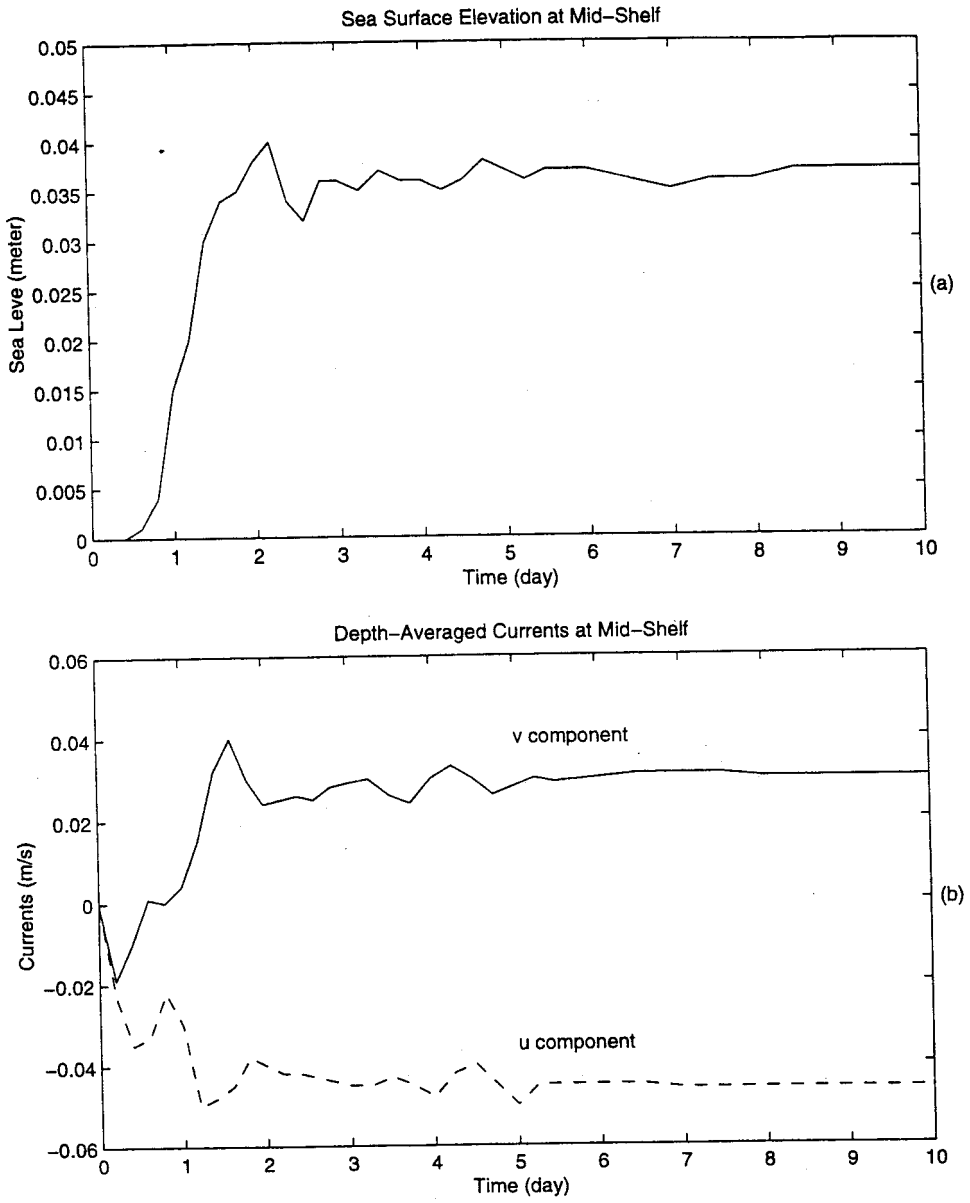

Figure 3. Model spin-up process of the continental shelf circulation driven by January wind stress. (a) Sea surface elevation time series and (b) depth averaged current time series at midshelf location. Sea surface elevation is in unit of meters and current is in unit of meters per second.

face wind stress is specified by the monthly mean wind stress climatology of *Hellerman and Rosenstein* [1983], linearly interpolated to fit the model grid.

2.2. Climatological Wind Stress

Located in the eastern Gulf of Mexico, the West Florida Shelf is influenced by the subtropical high-pressure pattern called the Bermuda High. In summer, when the Burmuda High is farthest north, the eastern Gulf of Mexico has prevailing southeasterly winds, whereas in winter, when the Bermuda High moves equatorward, an anticyclonic cell forms over the continent, producing northeasterly flow over the eastern gulf. Thus the circulation of the eastern Gulf is influenced in spring and summer by tropical air masses, arriving from the south and southeast and by subtropical or continental air masses in late fall and winter.

Examples of the climatological wind stress fields for the months of January and July are shown in Figure 2. During winter (Figure 2a), the northeasterly to northerly winds are relatively strong. Downcoast directed along-shelf wind stress is limited to the nearshore region over the Big Bend. Over the remainder of the shelf, the wind stress is mainly directed offshore. In contrast, during summer (Figure 2b), the winds are southeasterly. The along-shelf component of the wind stress therefore reverses over the shelf from winter to summer. Similar climatological wind stress fields for each of the

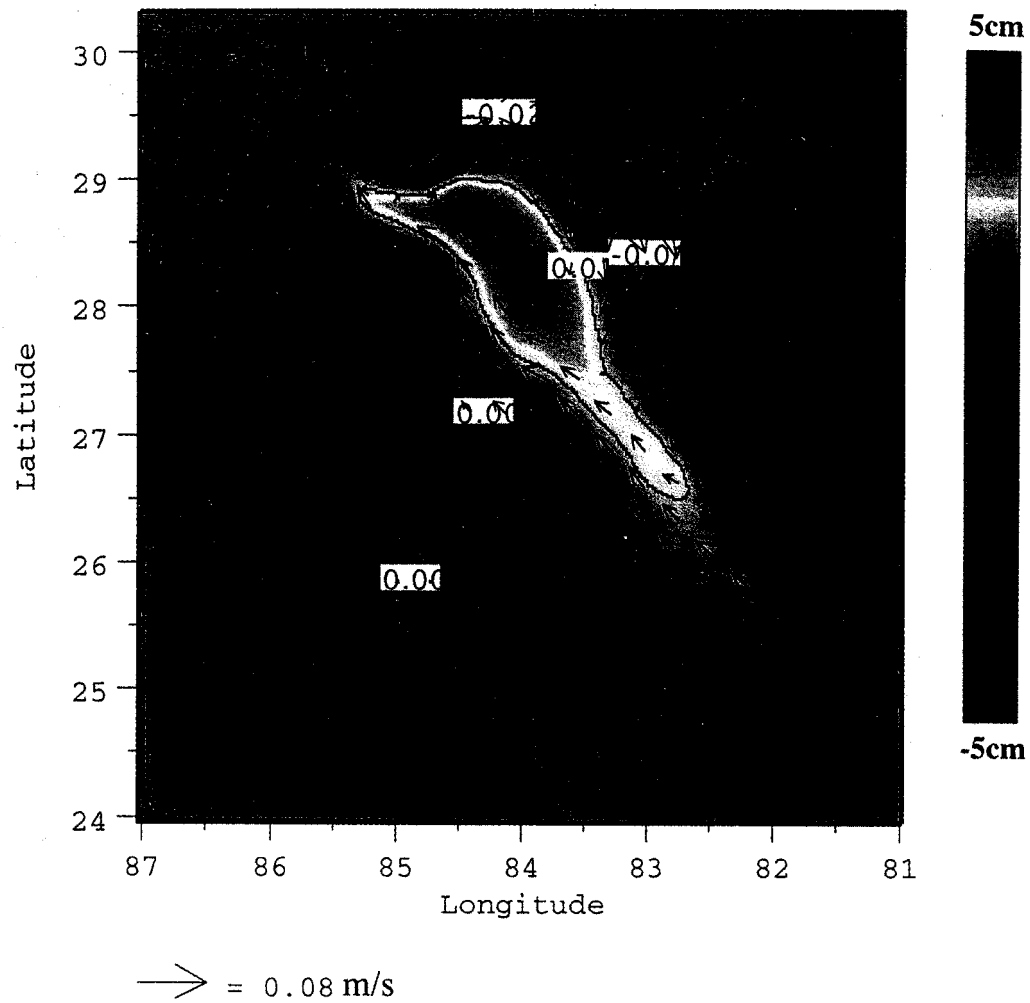

Plate 1. Model quasi steady depth-averaged current and the surface elevation perturbation pattern in January after a 20-day integration. The color scale presents the surface elevation perturbation. Solid lines are the surface elevation perturbation contour lines in units of meters. The arrows are for the current vectors in units of meters per second.

12 calendar months were used for the surface forcing fields in this study.

3. Main Results

3.1. Big Bend Gyre

The model spin-up from a state of rest using a constant density and the climatological January wind stress field is shown at a midshelf location in Figure 3. The sea surface elevation and currents reach a quasi steady state within 2 days, which is consistent with the finding of *Hsueh et al.* [1982]. The northeasterly wind drives water southwestward initially (within the first 6 hours or so) and then northwestward (after less than 2 days), causing a mass redistribution and a pressure adjustment. The result is a combined Ekman and geostrophic balance (shown in Figure 3a by the sea surface elevation). Thus the model spin-up time is essentially the time taken to set up the sea surface slope. Since Ekman dynamics provide a wind-driven transport to the right of the wind stress, the Ekman transport is northwestward in response to the northeasterly wind stress (see Figure 3b). Combined with the geostrophic transport, the resulting sea level and depth-averaged current patterns after a 20-day integration are shown in Plate 1. In response to a predominantly offshore wind in the south and southerly wind in the north, a sea level depression occurs near the coast and a related southeastward coastal jet emerges with a northwestward flow from the south to form an anticyclonic gyre within the northeastern Florida Big Bend region.

Dynamically, it is the along-shelf component of the wind stress that primarily produces the along-shelf flow. The water mass distribution then geostrophically adjusts to this along-shelf flow over the shelf, resulting in a geostrophically adjusted cross-shelf slope of the sea surface. In January (Figure 2a), the along-shelf component of the wind stress is southeastward in the northern

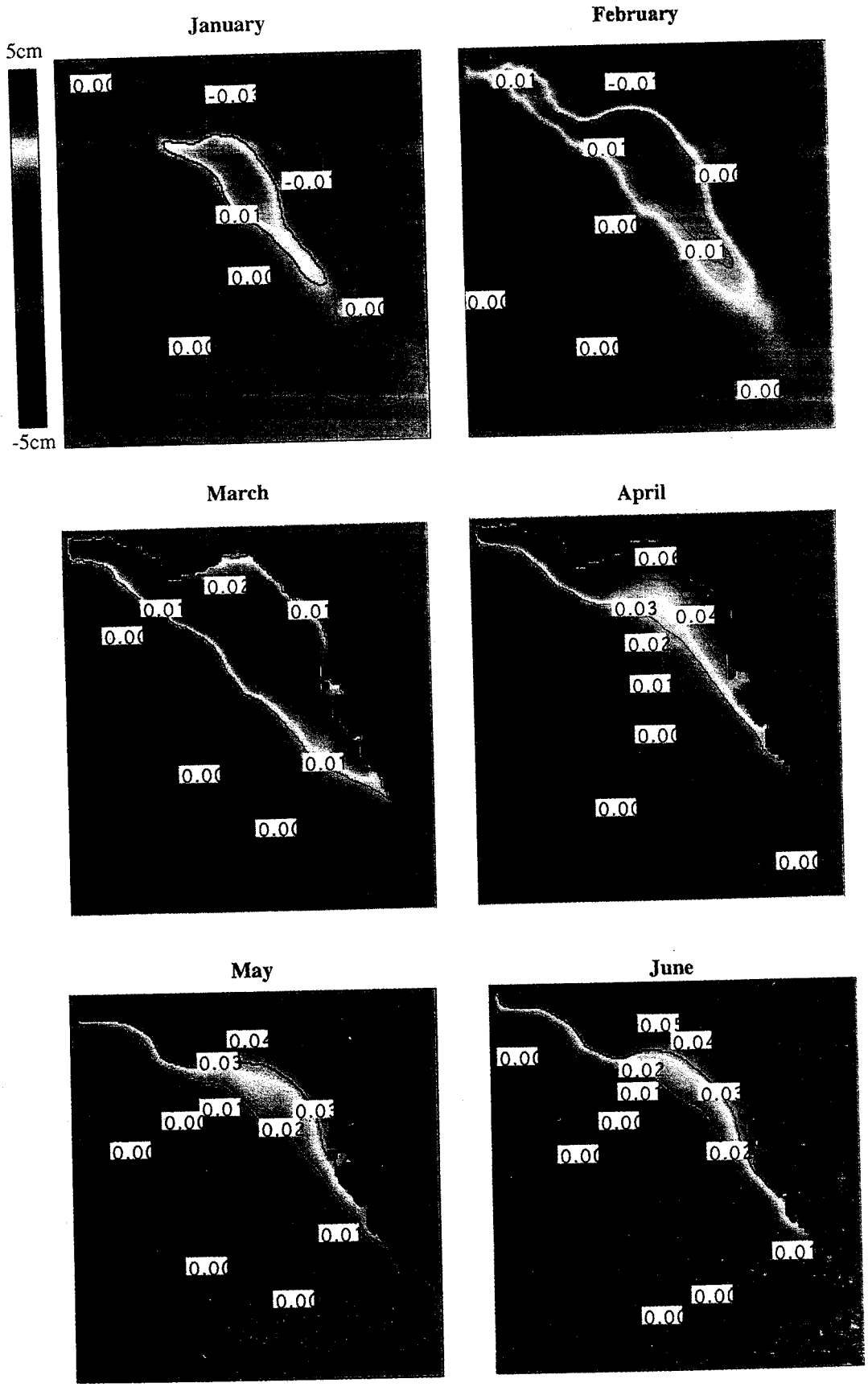

Plate 2. Model monthly sea surface elevation. Solid lines are the perturbation contour lines in units of meters. These plots have the same latitude and longitude configuration as in Figure.1

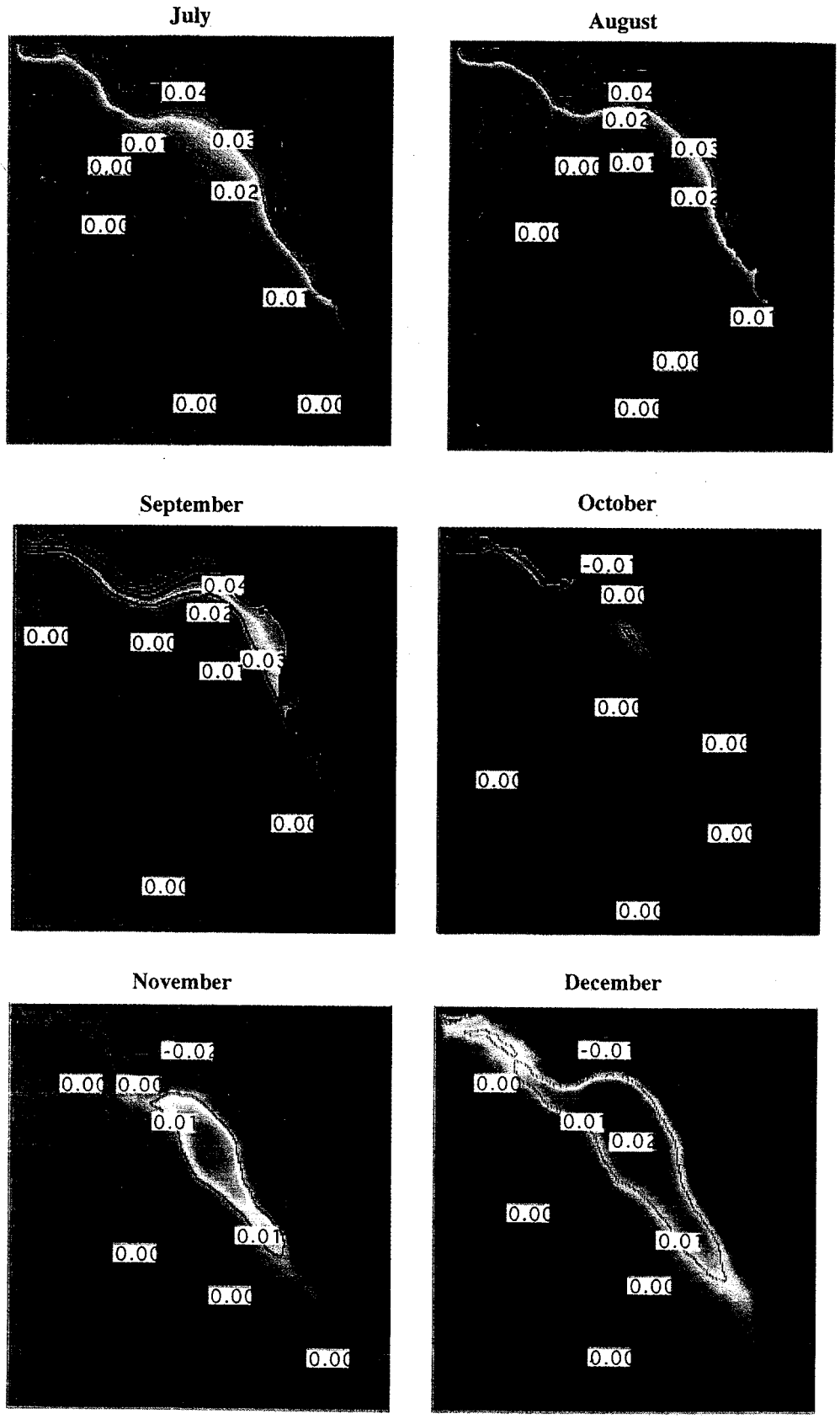

Plate 2. (continued)

region. This generates the southeastward along-shelf flow or the coastal jet and its geostrophically related across-shelf sea surface slope. However, this alongshelf wind stress is limited to the northern inner shelf region. Over the rest of the shelf, the wind stress is offshore, and this offshore wind stress induces a northwestward Ekman flow. The southeastward alongshelf flow and the northwestward Ekman flow converge over the central midshelf to produce an anticylonic gyre-like pattern, which we call the Big Bend Gyre.

One can demonstrate that on the continental shelf, local vorticity can be generated by two forcing mechanisms. One is the wind stress curl, and the other is the alongshore component of wind stress. We can show these processes as follows. Consider a coastline that, at least locally, may be taken to be straight at $x = x_e$. Suppose that in the region considered, the depth H of the ocean is a function only of distance from the coast, that is, $H = H(x)$. On the west coast of the continent, e.g., with the land to the east, H decreases eastward with an x increase. The inviscid, linearized, vertically integrated shallow water equations are

$$\frac{\partial u}{\partial t} - fv = -g\frac{\partial \eta}{\partial x} + \frac{X}{H}, \tag{8}$$

$$\frac{\partial v}{\partial t} + fu = -g\frac{\partial \eta}{\partial y} + \frac{Y}{H}, \tag{9}$$

where u and v are the depth-averaged components of velocity in the onshore and alongshore directions, respectively; and X and Y are the onshore and alongshore components of wind stress acting on the ocean surface, respectively, divided by the water density [*Gill and Schumann*, 1974]. Taking the x and y derivatives of the two equations and forming the vertical vorticity equation, we have

$$\frac{\partial \zeta}{\partial t} = -f\left(\frac{\partial u}{\partial x} + \frac{\partial v}{\partial y}\right) + \frac{1}{H}\left(\frac{\partial Y}{\partial x} - \frac{\partial X}{\partial y}\right) - Y\frac{dH}{dx}, \tag{10}$$

where $\zeta = \partial v/\partial x - \partial u/\partial y$ is the vorticity. The left-hand side is the local vorticity tendency, and the right-hand side provides the vorticity generation terms. There are two external forcing mechanisms: the wind stress curl and the alongshore component of the stress.

Generally, the second mechanism dominates over the first one. Thus it is alongshore wind stress that is effective at inducing the vorticity, which is cyclonic when the stress has an alongshore component with the land to the right and anticyclonic when the stress has alongshore component with the land to the left. The physical mechanism is simple. When the stress has an alongshore component with the land to the right, it produces an alongshore flow. However, as the water column becomes shallow toward the shore line, the alongshore flow increases in magnitude and induces a coastal jet. This cross-shore shear produces a cyclonic vorticity. Likewise, when the stress has an alongshore component with the land to the left, it produces an alongshore flow with shear of opposite sign and hence an anticyclonic vorticity. Figure 4 illustrates these mechanisms.

In the northern region of the West Florida Shelf, the wind stress has an alongshore component with the land to the left in winter. Thus it generates an anticyclonic vorticity tendency over the Big Bend region. Accordingly, the southeastward along-shore wind stress over the West Florida Shelf may be able to generate such an anticyclone. To test this idea, we ran the model forced by an unidirectional alongshore wind stress. The model, however, failed to generate such a Big Bend Gyre. Therefore the alongshore component stress alone is not sufficient to generate and maintain the Big Bend

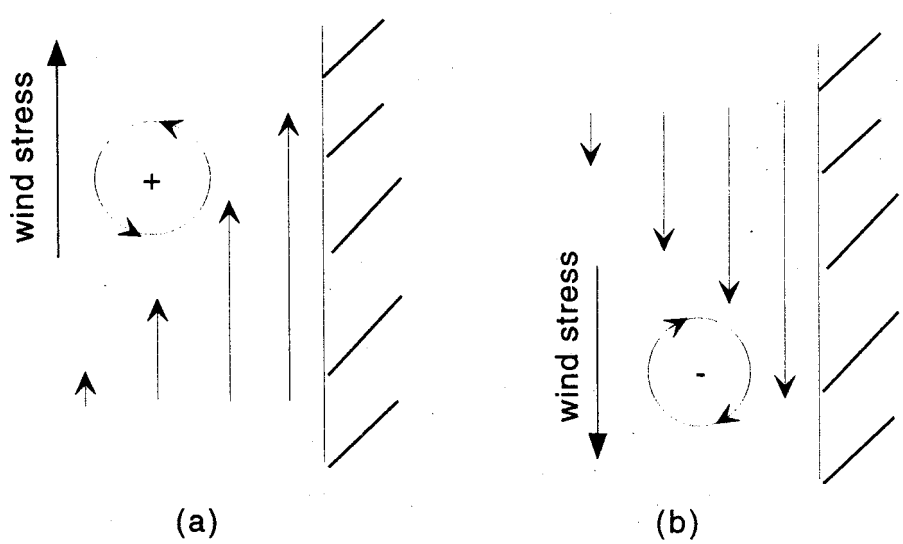

Figure 4. Schematic of the local vorticity and coastal jet generation by the alongshore component of wind stress. (a) Vorticity tendency is cyclonic when the wind stress has an alongshore component with the land to the right (b) Vorticity tendency is anticlyclonic when the stress has an alongshore component with the land to the left. In both cases, a coastal jet can be generated.

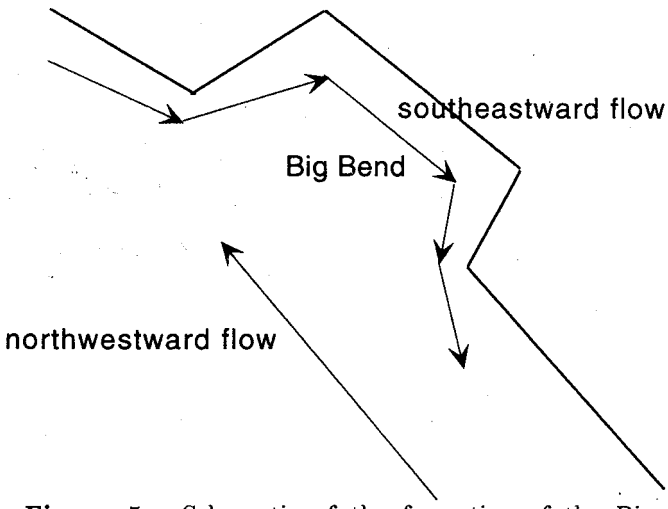

Figure 5. Schematic of the formation of the Big Bend Gyre due to the convergence of two flows. The southeastward alongshelf component of wind stress in the northern inner shelf generates the anticyclonic vorticity tendency and southeastward directed coastal jet whereas the alongshelf component of wind stress in the south and offshore produces a northwestward flow.

Gyre. It is combination of the alongshore wind stress near the shore in the north and wind stress as it turns offshore over the rest of the shelf that produces the Big Bend Gyre. In essence, it is the convergence of two flows over the Big Bend region as depicted in Figure 5 that provides the possible mechanism for the generation and maintenance of the Big Bend Gyre in the model. In Figure 5, the southeastward alongshelf wind produces a negative vorticity tendency over the shelf and a coastal jet. The wind stress in the north and offshore produces a northwestward flow. The two flows meet in the north and result in the Big Bend Gyre.

3.2. Depth-Averaged Circulation and Sea Level

Using monthly climatological wind stress and constant density, 12 separate numerical experiments were conducted, one for each month. The quasi-steady sea surface elevation patterns after a 20-day integration are presented in Plate 2 and the corresponding depth-averaged circulation patterns are given in Figure 6. The annual variations of the West Florida Shelf circulation in response to the annually varying climatological wind fields are clearly evident, particularly in the annual reversals of the circulation over the Florida Big Bend region and the coastal sea surface elevation changes. Two basic shelf circulation and sea surface elevation patterns emerge: a winter pattern from October to March, and a summer pattern from April to September, with transitional patterns in between.

In late fall and winter, the along-shelf component of the wind stress is southeastward in the northern region. This generates a southeastward along-shelf flow and a geostrophically adjusted coastal jet (Figure 6), manifest in the across-shelf slope of the sea surface and the set down of sea level at the coast (Plate 2). However, this along-shelf wind stress is limited to the northern inner shelf. Over the rest of the shelf, the wind stress is offshore. This offshore wind stress induces a northwestward Ekman flow. The southeastward along-shelf flow and the northwestward Ekman flow converge over the central mid-shelf producing the anticylonic gyre-like pattern (Plate 2). This gyre joins a relatively strong, northwestward directed jet centered approximately along the 50 m isobath at midshelf.

In summer, the alongshelf component of the wind stress is northwestward and it induces a northwestward flow. The associated geostrophically adjusted sea surface level decreases offshore over the entire shelf. The reason the shelf circulation structure is simpler in summer than in winter is that during summer the wind stress is weak and almost unidirectional toward the northwest.

In spring, the Bermuda High moves back toward the north. The winds over the West Florida Shelf change from northeasterly to easterly and southerly, and the anticyclonic gyre over the northeastern Florida Big Bend region disappears. Coastal sea surface elevation increases and peaks in late summer. The resulting elevated coastal sea surface results in a continuous northwestward coastal jet along the entire West Florida Shelf. The jet is strongest along the Florida panhandle, where the isobaths converge. This pattern persists into September.

The transitional seasons therefore show either development (in late fall) or relaxation (in spring) of the Big Bend Gyre and its associated circulation patterns. The coastal jet along the Florida panhandle, however, appears 1 month earlier in spring and 1 month later in winter. For example, even though the Florida Big Bend Gyre and the associated fall-winter circulation pattern appear as early as October, the Florida panhandle coastal jet is still in the summer pattern. Similarly, in March the circulation pattern is still in the winter pattern, but the coastal jet is already in the spring-summer pattern.

The seasonal change in the coastal sea level is clearly one of the major features in these experiments. These model results show that, in general, the coastal sea level is relatively high in the summer and low in the winter (Plate 2). However, the annual variability differs greatly from the Florida Keys to the Florida Big Bend and the Florida panhandle, and this variability generally increases from south to north. For example, while there is no appreciable seasonal change in the Florida Keys, the annual change is as big as 12 cm in the north. The sea level reaches its maximum in April and September and minimum in January.

3.3. Vertical Structure of Shelf Circulations

The vertical structure of modeled shelf circulation patterns are shown in Figure 7 at sigma levels 1 (sur-

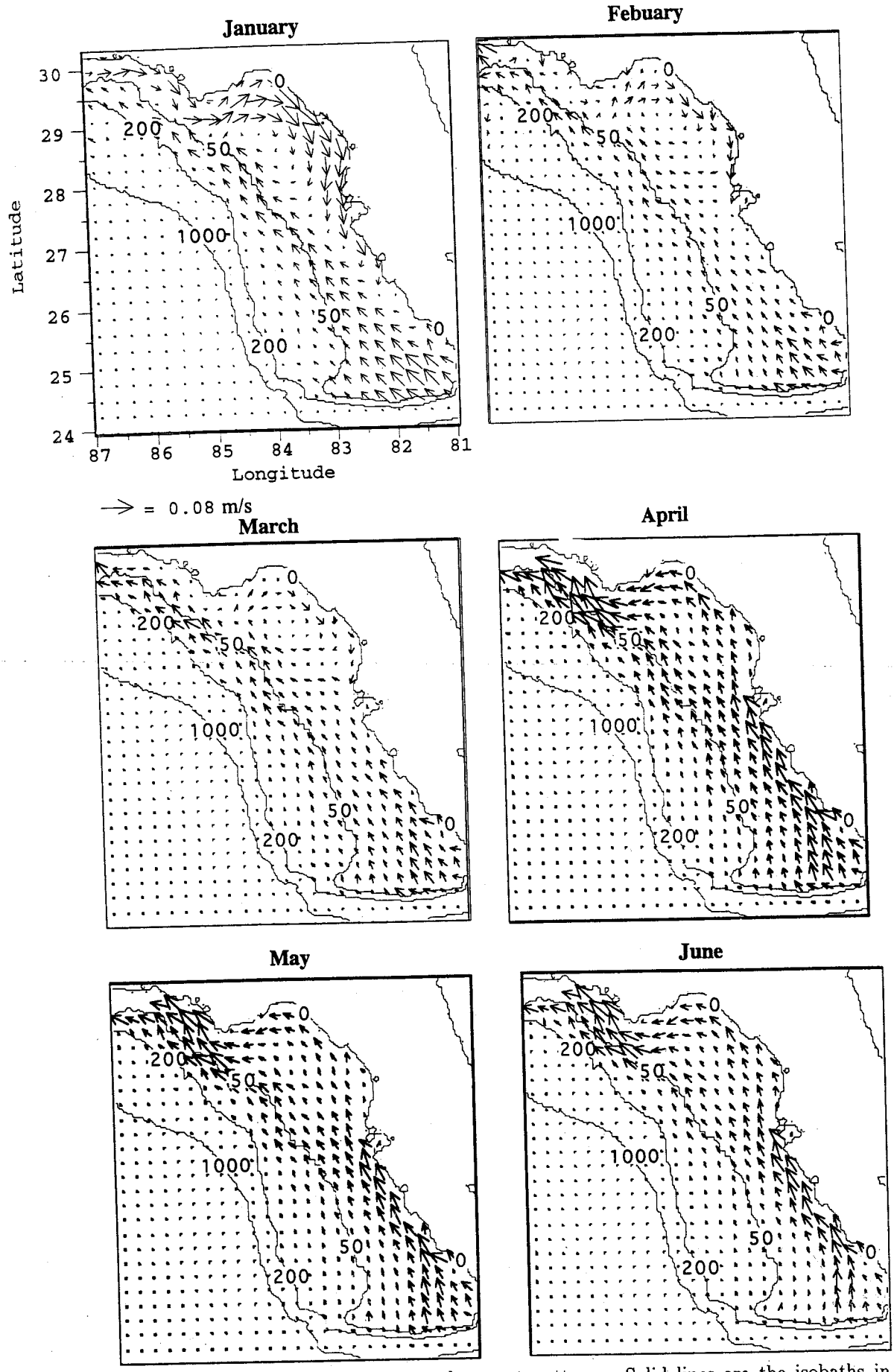

Figure 6. Model monthly depth-averaged current patterns. Solid lines are the isobaths in meters. These plots have the same latitude and longitude configuration as in Figure 1, and the scale is the same as in Plate 1.

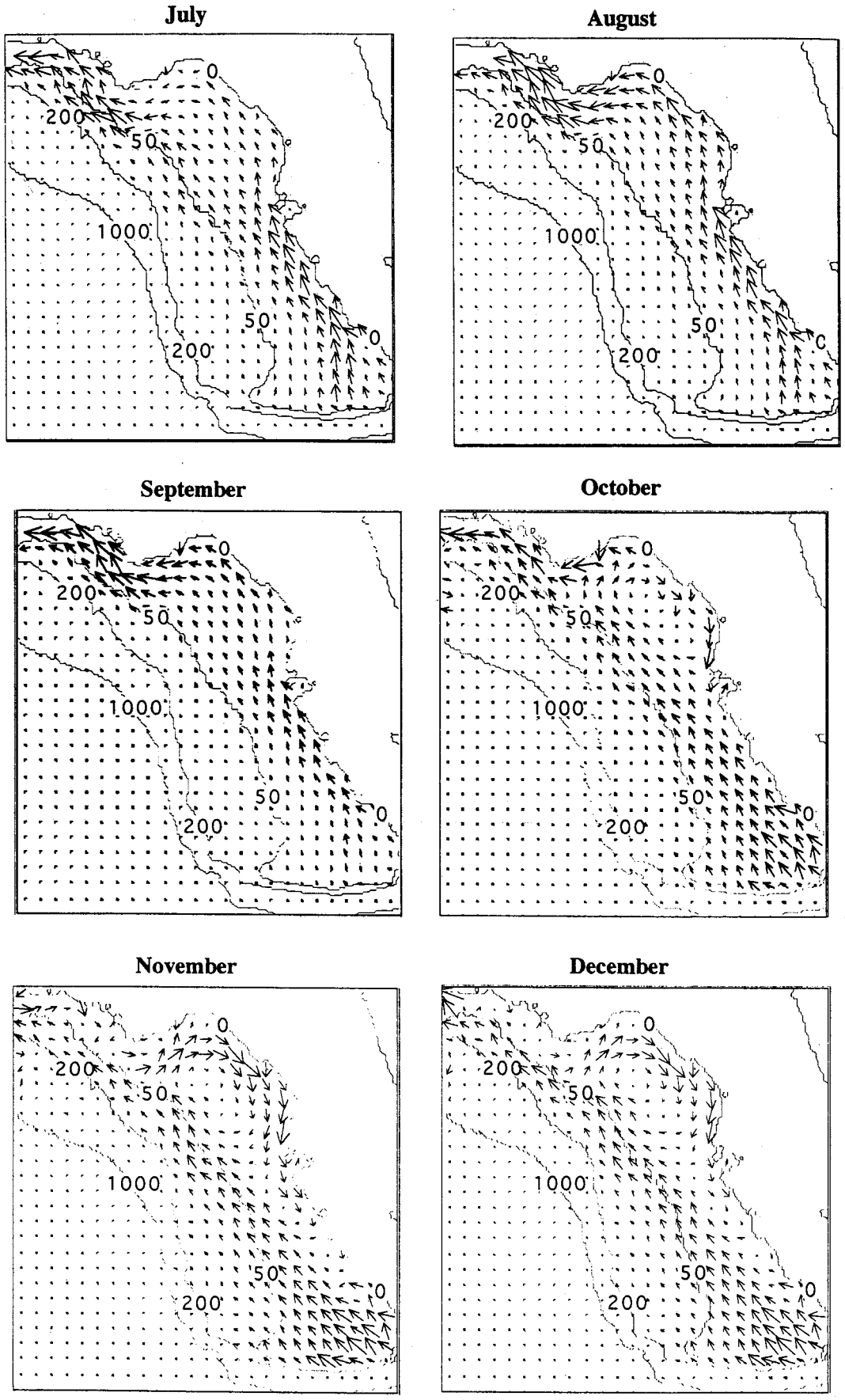

Figure 6. (continued)

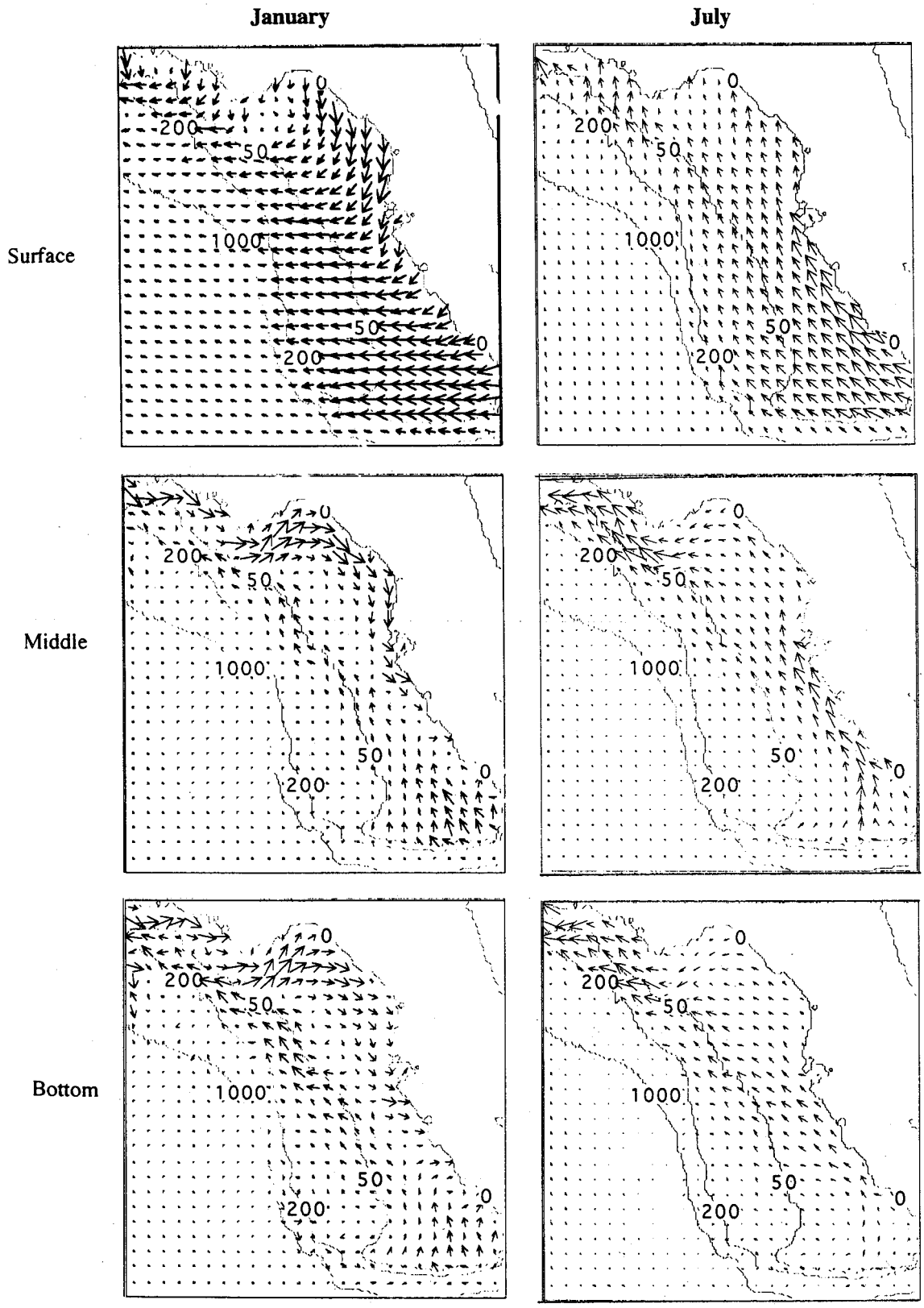

Figure 7. Vertical structure of model horizontal circulation patterns in (left) January and in (right) July, showing (top) the surface current (on sigma level 1), (middle) the middepth current (on sigma level 11), and (bottom) the near-bottom current (on sigma level 20). These plots have the same latitude and longitude configuration as in Figure 1.

face), 11 (middepth) and 20 (near bottom) for winter (January) and summer (July) months. In winter, coastal surface currents tend to be in the direction of wind stress because of direct wind forcing. Farther offshore, the surface currents tend to be at a 45° angle to the right of the wind stress, in accordance with Ekman dynamics. At sigma level 11, the middepth currents are similar to the vertical average as discussed above. A relatively strong southeastward directed flow also appears inside the 20 m isobath. This coastal jet occurs because offshore transports in the surface circulation depress the coastal sea level; in turn, the coastal depression induces a southeastward directed coastal jet by geostrophic dynamics. Farther offshore from midshelf, as the depth increases, current vectors veer to the right near the surface, also in accordance with Ekman dynamics. They gradually align with the bathymetry at depth. At sigma level 20, the near bottom currents decrease in magnitude and veer to the left of the middepth currents. A northwestward directed flow with a center line along the 50 m isobath exists in midshelf at both the middle and nearbottom sigma levels.

In summer, the alongshore currents are all directed northwestward in the inner shelf and the coastal jet becomes a continuously salient feature because the anticyclonic gyre over the Florida Big Bend region disappears. The inner shelf across-shore current is directed onshore near the surface and offshore at middepth and near the bottom. Thus the seasonal reversals that occur from January to July include the direction of the coastal jet, its associated sea level, and the onshore and offshore transports, which, in turn, induce upwelling and downwelling, respectively.

3.4. Upwelling and Downwelling

The vertical velocity normal to the sigma surface ω and the onshore or offshore horizontal transports along the sloping topography contribute to the vertical motion in the z direction. Vertical motions in the z direction are called upwelling or downwelling and Figure 8 shows the model results near the bottom for January and July. January is characterized by three distinct regions (Figure 8a): an upwelling region onshore from the midshelf (50 m isobath), a downwelling region offshore from the midshelf; and the shelf break region with alternating up and down motion. These upwelling and downwelling regions are controled by the offshore or onshore horizontal transports along the sloping shelf topography. July, in contrast, is characterized by two regions (Figure 8b): a downwelling region over most of the shelf, and the shelf break region with alternating up and down motion. Therefore an annual reversal of the vertical motion occurs over the inner shelf.

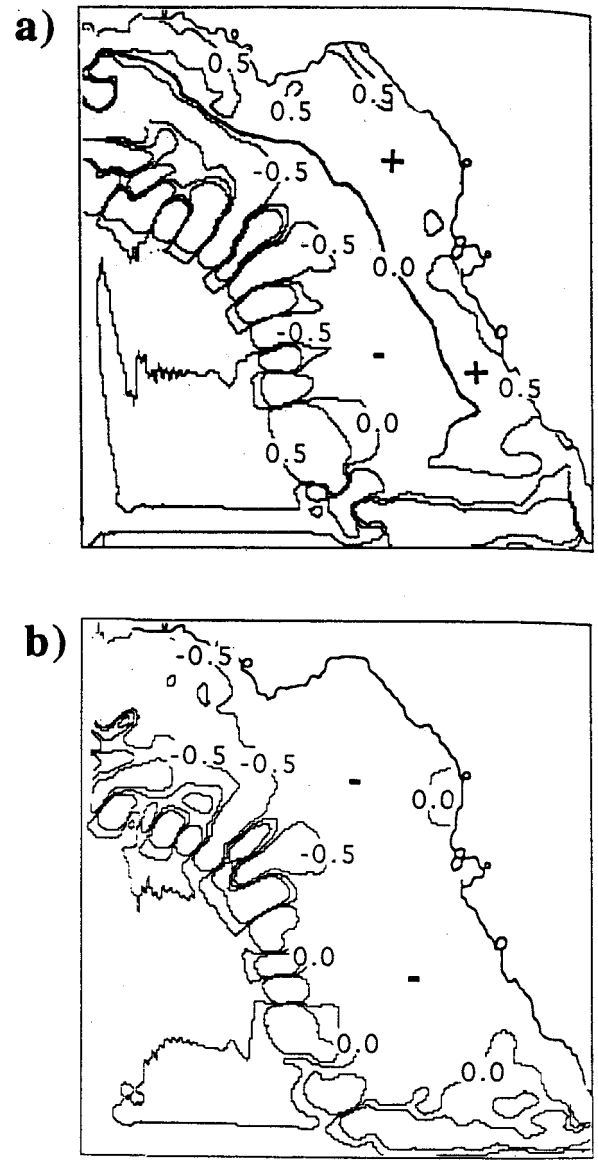

Figure 8. Model vertical velocity in z direction near the bottom in units of 10^{-5} meters per second in (a) January and (b) July. These plots have the same configuration as that in Figure 1. The pluses and minuses denote the upward and downward motions, respectively.

4. Data Comparison

By design, the above experiments excluded the Loop Current and density-related effects. Since these factors are important for the shelf circulation near the shelf break and vertical stratification increases in summer, our model results are most relevant for the inner shelf during winter. However, our goal is not a realistic simulation of the shelf circulation, rather, an investigation of how the shelf may respond to seasonal wind forcing alone.

4.1. Recent in Situ Current Data

Two relatively long term in situ current data sets at midshelf have resulted from recent mooring deployments (Figure 1). One derives from a surface mounted acoustic Doppler current profiler (ADCP) at 28°N, 84°W, labeled USF1, for the period of October 1993 to January 1995 [*Weisberg et al.*, 1996]; and the other is from

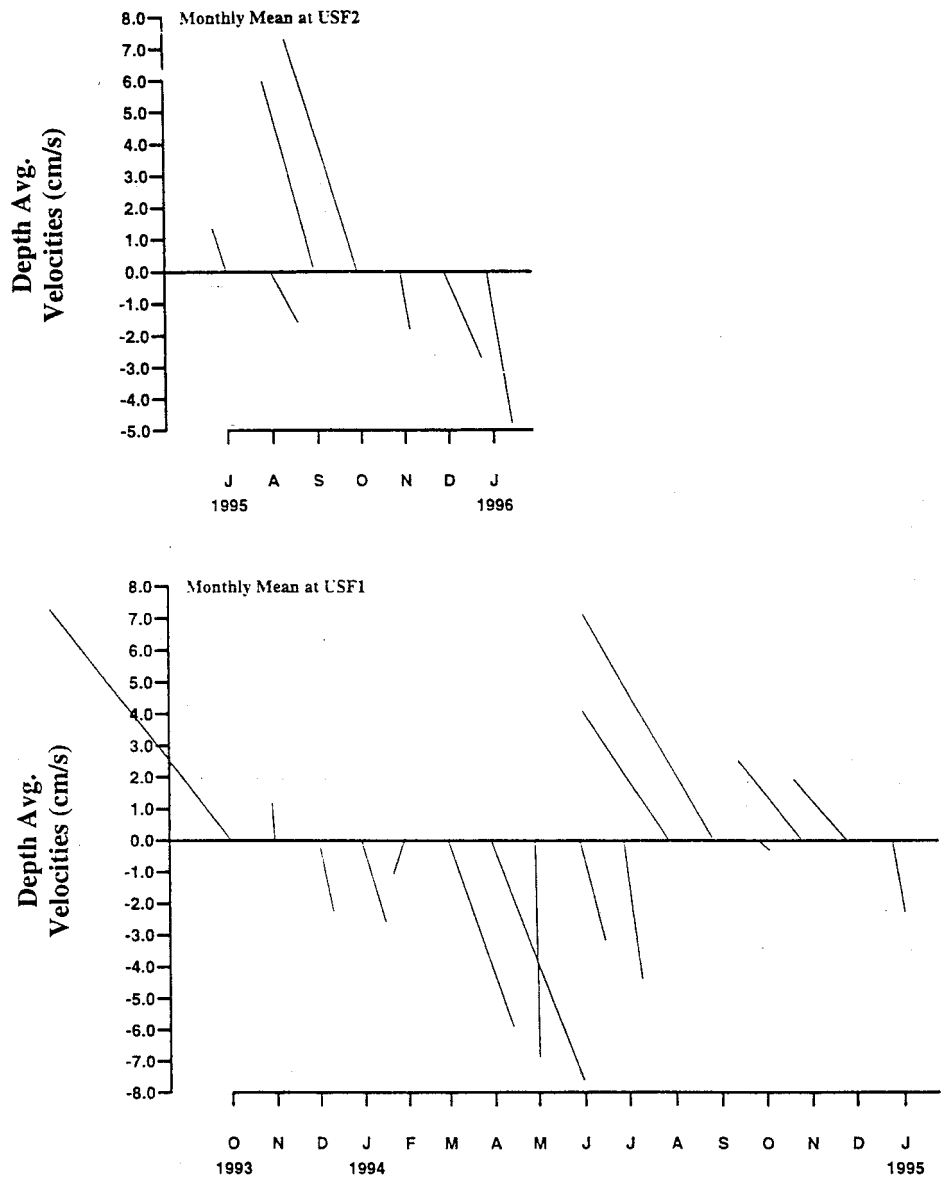

Figure 9. Monthly mean depth-averaged in situ observations at USF1, located at 28°N, 84°W, from October 1993 to January 1995; and at USF2, located at 27°49'N, 83°25'W, from July 1995 to January 1996.

a subsurface mounted ADCP at 27°49'N, 83°25'W, labeled USF2, for the period of July 1995 to January 1996. Figure 9 gives the monthly mean depth-averaged currents from both locations. A seasonal reversal of the alongshore transport is evident in these midshelf data. The transports at both sites tend to be alongshore, but reversing from upcoast in late summer and fall to downcoast during the remainder of the year. Figure 10 shows corresponding model depth-averaged currents at a Clearwater coastal location and at the USF2 and USF1 sites (Figure 1).

These in situ current observations are too short to represent the climatological condition at the midshelf and too sparse to resolve the spatial features observed in the modeling results. Despite these shortcomings, the model results at the USF2 site capture a seasonal reversal that depends upon offshore position. In this sense, a qualitative agreement is achieved. However, for the region farther offshore, the reversal is not evident in the model, which suggests that some relevant physical factors are missing in the model.

4.2. Drifter Data

Lagrangian-like drifters provide very important information about the shelf circulation, even though they are far from perfect. Results from two drifter studies are available for the region. The first derives from drift bottle data during the Hourglass program [*Williams et al.*, 1977] and the second is from satellite tracked drifters deployed during a recent Minerals Management Service (MMS) program [*P. P. Niller et al.*, personal communication, 1996). The Hourglass data come from a se-

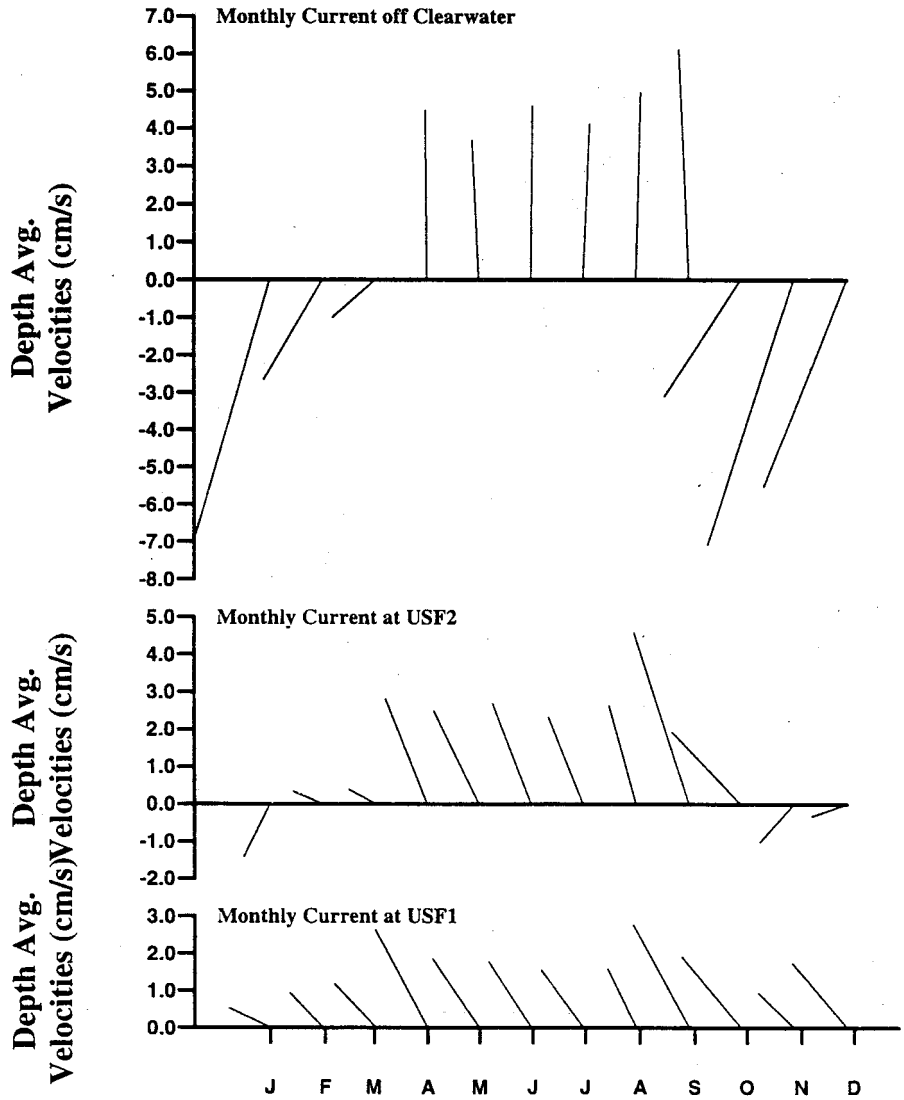

Figure 10. Model monthly depth-averaged currents at the off-Clearwater coastal location, USF2 and USF1. A seasonal reversal of circulation direction is indicated at the USF2 site and the off-Clearwater location.

ries of cruises on the continental shelf between Tampa Bay and Fort. Myers during 28 months from August 1965 to November 1967 (Figure 1). Drift bottles were released at each station to study the surface circulation. A total of 4460 drift bottles were released with 32% retrieval rate. These data are summarized in Table 1. More than 80% of the retrieved drift bottles were found to eventually flow southward over the shelf during fall and winter months from November to March. For example, during January and February, all drifters were found to the south, and only 11%, 17% and 19% of the retrieved drift bottles were found to the north in December, March, and November, respectively. In contrast, more than 40% of the retrieved drift bottles were found north of their deployment sites from April to September. For example, 53%, 57% and 52% of the retrieved drift bottles were found to the north in July, August, and September, respectively. This suggests a seasonal variability in the surface shelf circulation and a possible seasonal reversal of the net transport direction.

Accordingly, Figure 11 shows the surface circulation patterns from the model results. From April to

Figure 11. Model monthly surface shelf circulation patterns, showing an offshore surface transport during the period from October to March and a northwestward and an onshore surface transport during the period from April to September over the central and southern West Florida Shelf. These plots have the same latitude and longitude configuration as in Figure 1.

January
February
March
April
May
June
July
August
September
October
November
December
30
29
28
27
26
25
24
−86
−84
−82

Table 1. Percentage of Retrieved Drift Bottles That Flow to North and South, Based on the Hourglass Drift Bottle Data

	North	South
Jan.	0	100
Feb.	0	100
Mar.	17	83
Apr.	46	54
May	48	52
Jun.	41	59
Jul.	53	47
Aug.	57	43
Sep.	52	48
Oct.	28	72
Nov.	19	81
Dec.	11	89

Data are based on *Williams et al.* [1977].

September, the surface shelf circulation is predominantly northwestward alongshore and onshore. Therefore the model results are consistent with the Hourglass drift bottle retrievals found to the north. In contrast, from October to March, the surface shelf currents are offshore over most of the shelf. It is well understood that there is a southward directed flow off the shelf break due to the Loop Current, particularly in the southwest region. Assuming that over the southwest continental shelf, offshore surface currents result in drifters moving into the southward directed Loop Current (which is not included in the model), then the model results have the following implications: from October to March, the offshore surface currents may bring the surface drifters farther off the shelf break and into the Loop Current. In turn, the Loop Current may eventually drive the drifters to the south. Therefore the model results are also consistent with those found to the south if we invoke an offshore transport that leads to entrainment by the Loop Current.

The MMS drifter data provide a more detailed description of the surface Lagrangian circulation for the West Florida Shelf during February 1996 to May 1997. While these data are in their initial stages of analysis they also imply a seasonality to the West Florida Shelf circulation [*P. P. Niller et al*, personal communication, 1996].

4.3. Tide Gauge Data

While the dominant variance of the coastal water level variations in the synoptic band (roughly 2 day to 2 week periodicity) is well explained by the wind on the West Florida Shelf [*Mitchum and Clarke*, 1986], it is not so for the annual cycle. Even though the annual cycle has contributions from both the annual thermosteric changes in the water column and atmospheric pressure, the across-shelf slope of the sea surface may be related to the wind forcing, to some extent. The wind-induced contribution to the cycle may still be significant.

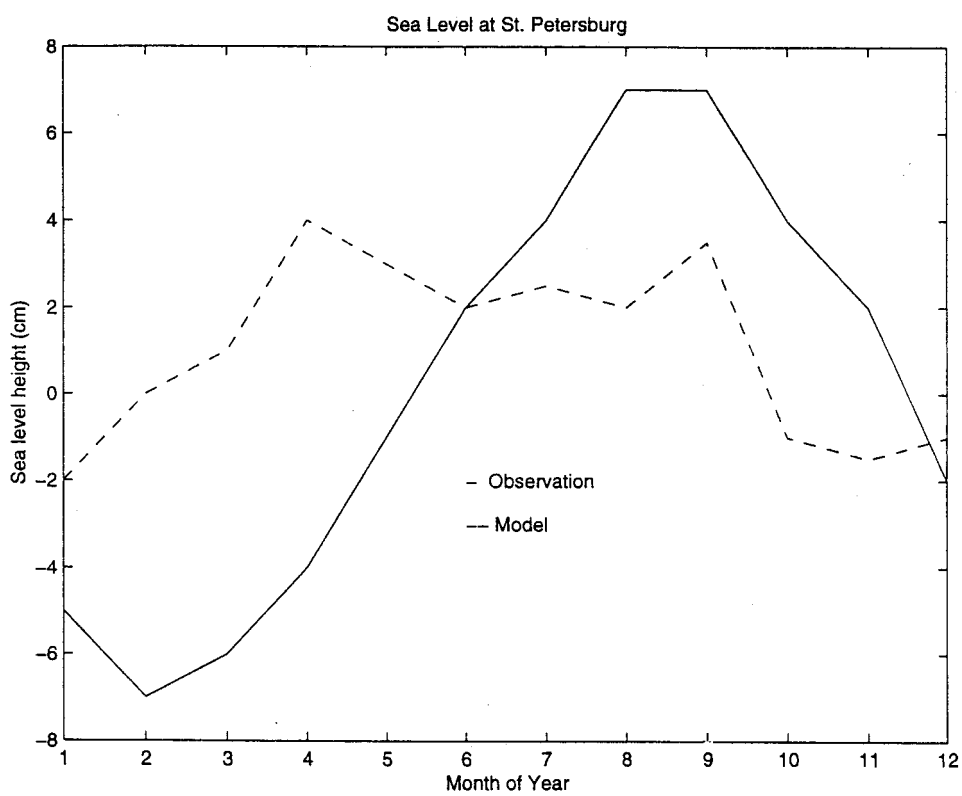

Figure 12. Model and observed monthly sea level heights at St. Petersburg.

The model results (Figure 12) show that there is an annual change in the coastal sea surface elevation. The elevation reaches its maximum in April and September and its minimum in January. This annual change increases from south to north. These results are generally consistent with observations [*Blaha and Sturges*, 1981]. For example, both the model and observations show relatively little sea level change at Key West. The observed annual change of sea surface elevation in St. Petersburg is about 16cm with the highest in September and the lowest in February. The model results show a 6cm annual sea level change. The observed annual sea level change at Pensacola is about 20 cm [*Blaha and Sturges*, 1981], whereas the model result is 8 cm at Cedar Key and as high as 9 cm near Apalachicola. Monthly wind climatology therefore accounts for about one third of the total sea level change at St. Petersburg and a larger fraction at the Florida panhandle coast. The rest may be due to both steric and atmospheric pressure effects. Therefore, the seasonal change of sea surface level along the coast suggests a direct link between the wind and the sea level change shown in many previous studies [*Blaha and Sturges*, 1981; *Mitchum and Sturges*, 1982; *Mitchum and Clarke*, 1986]. However, this linkage is not necessarily a local one because the model includes both the shelf-wide and local impacts of the wind [*Mitchum and Clarke*, 1986]. It is also clear from our model study that not only the alongshore wind is important; the across-shore wind contributes to the coastal sea level change. For example, the offshore wind in the southern region (Figure 2a) produces a relatively low sea level near the coast (Plate 1).

5. Summary

The response of the west Florida continental shelf circulation to monthly mean climatological wind forcing was investigated by using a three-dimensional, primitive equation numerical ocean model. Two basic seasonal patterns of circulation and sea level emerge: a winter pattern from October to March and a summer pattern from April to September. The winter pattern consists of an anticyclonic gyre over the northeastern (Florida Big Bend) region that joins a northwestward directed flow from the south. This pattern is characterized by relatively low coastal sea level, offshore surface transport, and coastal upwelling. The summer pattern has a continuous northwestward directed flow, relatively high coastal sea level, onshore surface transport, and coastal downwelling. The transitional seasons display either the development or relaxation of the anticyclonic gyre over the Florida Big Bend region. These circulation patterns result from wind-driven Ekman transports and the resulting surface-slope-induced geostrophic flows. The Big Bend Gyre is one of the most interesting findings of this study in winter. The generation of this gyre is due to the convergece of two wind-driven flows, one from the inner shelf in the north and the other from offshore over the rest of the shelf. Model results are in qualitative agreement with recent in situ current observations, historic drift bottle retrievals, and tide gauge data. The across-shelf transports and their related coastal upwelling and downwelling may greatly influence the distributions of continental marine materials with biological and geochemical importance for the West Florida Shelf environment. However, climatological wind stress forcing alone does not account for the seasonal reversal in currents found at midshelf. It is therefore concluded that one can reasonaably treat the depth-averaged flow as governed by wind stress within 50 m depth contour based on the present study, and beyond this limit, seasonal density effects must also be an important factor in the seasonally varying circulation on the West Florida Shelf.

To explore this assertion, a similar set of numerical experiments was performed with the *Levitus* [1982] temperature and salinity climatology in attempt to account for baroclinic effects. This climatological density field, while vertically stratified, is almost horizontally uniform. It limited the circulation to the upper layer in a very unrealistic way while failing to improve upon seasonal variation. However, the density field, especially its horizontal gradient, is likely to be very important in determining the seasonal variation in the shelf circulation as implied by remotely sensed satellite sea surface temperature data and in situ observations. Resolving the seasonally varying shelf circulation, particularly the southward directed flow observed at midshelf over a large portion of the year, may require serially and synoptically sampled hydrographic data tied into several absolute sea level points.

Acknowledgments. This work was supported by the USGS Center for Coastal Geology, St. Petersburg, Florida as part of the West-Central Florida Coastal Erosion Study. Additional support is from the Minerals Management Service as part of the Northeastern Gulf of Mexico Circulation Study. We appreciate the many constructive comments by one of our reviewers that helped to clarify discussion of the anticyclonic gyre. The data analysis assistance by Bryan Black and the editorial assistance by Kristen Kusek and Jyotika Virmani are also appreciated.

References

Blaha, J. and W. Sturges, Evidence for wind-forced circulation in the Gulf of Mexico. *J. Mar. Res.*, *39*, 711-733, 1981.

Blumberg, A. F. and G.L. Mellor, Diagnostic and prognostic numerical circulation studies of the South Atlantic Bight. *J. Geophy. Res.*, *88*, 4579-4592, 1983.

Blumberg, A. F. and G.L. Mellor, A description of a three-dimensional coastal ocean circulation model in *Three-Dimensional Coastal Ocean Models, Coastal Esturine Stud.*, *4*, edited by N. Heaps, 1-16, AGU, Washington, D.C., 1987.

Clarke, A. J. and K. H. Brink, The response of stratified, frictional flow of shelf and slope waters to fluctuating large-scale, low-frequency wind forcing, *J. Phys. Oceanogr.*, *15*, 439-453, 1985.

Cooper, C. K., A numerical modeling study of low-frequency circulation on the West Florida Shelf, *Coastal Engineering, 11*, 29-56, 1987.

Cragg, J., G. Mitchum and W. Sturges, Wind-induced sea surface slopes on the West Florida Shelf, *J. Phys. Oceanogr., 13*, 2201-2212, 1983.

Hellerman, S. and M. Rosenstein, Normal monthly wind stress over the world ocean with error estimates, *J. Phys. Oceanogr., 13*, 1093-1104, 1983.

Hsueh, Y., G.O. Marmorino and L.L. Vansant, Numerical model studies of the winter-storm response of the West Florida Shelf, *J. Phys. Oceanogr., 12*, 1037-1050, 1982.

Gilbes, F., C. Tomas, J.J. Walsh and F. E. Muller-Karger, An episodic chlorophyll plume on the West Florida shelf, *Cont. Shelf Res., 16*, 1201-1224, 1996.

Gill, A.E. and E.H. Schumann, The generation of long shelf waves by wind, *J. Phys. Oceanogr., 4*, 83-90, 1974.

Koblinsky, C.J., The M_2 tide of the West Florida Shelf, *Deep Sea Res., 28A*, 1517-1532, 1981.

Levitus, S., Climatological atlas of the world ocean, *NOAA Prof. Pap. 13*, U.S. Gov. Print Offi., Washington, D.C., 1982.

Marmorino, G.O., Wind-forced sea level variability along the West Florida Shelf, *J. Phys. Oceanogr., 12*, 389-404, 1982.

Maul, G., The annual cyclone of the Gulf Loop Current. Part I: Observations during a one year time series. *J. Mar. Res., 35*, 29-47, 1977.

Mellor, G.L. and T. Yamada, Development of a turbulence closure model for geophysical fluid problems, *Rev. Geophys. Space Phys., 20*, 851-875, 1982.

Mitchum, G.T. and W. Sturges, Wind-driven currents on the West Florida Shelf, *J. Phys. Oceanogr., 12*, 1310-1317, 1982.

Mitchum, G.T. and A.J. Clarke, Evaluation of frictional, wind-forced long waves theory on the West Florida Shelf, *J. Phys. Oceanogr., 16*, 1029-1037, 1986.

Niiler, P.P., Observations of low-frequency currents on the West Florida continental shelf, *Mem. Soc. R. Sci. Liege X, 6*, 331-358, 1976.

Oey, L.-Y., Eddy- and wind-forced shelf circulation, *J. Geophys. Res., 100*, 8621-8637, 1985.

Orlanski, I., A simple boundary condition for unbounded hyperbolic flows, *J. Comput. Phys., 21*, 251-269, 1976.

Steidinger, K.A, A re-evaluation for toxic dinoflagellate biology and ecology, *Prog. Phycological Res., 2*, 147-188, 1983.

Tolbert, W.H. and G.G. Salsman, Surface circulation of the eastern Gulf of Mexico as determined by drift-bottle studies, *J. Geophys. Res., 69*, 223-230, 1964.

Vargo, G.A., K.L. Carder, W. Gregg, E. Shanley and C. Heil, The potential contribution of primary production by red tides to the West Florida Shelf ecosystem, *Limnol. and Oceanogr., 32*, 762-767, 1987.

Weisberg, R.H., B.D. Black, and H. Yang, 1996: Seasonal modulation of the West Florida continental shelf circulation, *Geophys. Res. Lett., 23*, 2247-2250, 1996.

Williams, J., W.F. Grey, E.B. Murphy, and J.J. Crane, Memoirs of the Hourglass cruises, Rep. *IV*(III), Mar. Res. Lab., Fla. Dep. of Nat. Res., St. Petersburg, 1977.

H. Yang (corresponding author) and R. Weisberg, Department of Marine Science, University of South Florida, 140 7th Avenue South, St. Petersburg, FL 33701. (e-mail: yang@marine.usf.edu)

(Received September 29, 1997; revised July 7, 1998; accepted November 4, 1998.)